# Microwave Irradiation with Submerged Ultrasonication: A Novel Lignocellulosic Pretreatment Method

Rylan Q. Donohoe and Julia A. Seymour

Department of Science, St. Ignatius of Loyola Catholic Secondary School

## Author Note

Rylan Q. Donohoe https://orcid.org/0000-0002-7976-7997

Julia A. Seymour https://orcid.org/0000-0001-9373-2558

We have no known conflict of interest to disclose.

Correspondence concerning this article should be addressed to Rylan Q. Donohoe. Email: rylan.donohoe.287@loyola.hcdsb.org

**Abstract**

Starch-derived biofuels from first-generation feedstocks, like *Zea mays* (corn) and *Saccharum officinarum* (sugarcane), dominate the bioenergy market. The competing applications of these conventional sources of bioethanol present a sustainability issue. As the most abundant bioresource on Earth, lignocellulosic biomass (LCB), including most crop residues and herbaceous biomass, would be a superior source if only its conversion to ethanol were as efficient as that of starch-based feedstock. The recalcitrant molecular structure of LCB thwarts its industrial potential by hindering its enzymatic breakdown and subsequent fermentation. To enhance the efficiency and sustainability of this conversion process, a novel pretreatment method was devised using the synergistic properties of microwave (MW) and ultrasonic (US) irradiation. Corrugated fibreboard was used as an experimental feedstock to test 36 combinations of selected values for these variables. Following hydrolysis and fermentation, the resulting bioethanol concentration of each sample was quantified using an electronic sensor. The combination of 440 W of MW power (2,450 MHz, 8 min) and 480 s of submerged US irradiation (42 kHz, 35.00 W) yielded an optimal recovery of 2.24 ± 0.05% v/v of ethanol. A thin-plate spline curve fitting of all the collected data revealed a theoretical peak concentration of 2.26 ± 0.05% v/v from 500 W of MW power and 462 s of submerged US irradiation. This optimal combination recovers an additional 0.53% v/v of bioethanol compared to untreated LCB and an additional 0.06% v/v compared to untreated starch derivatives which have historically prevailed by 0.50% v/v. This increase in bioethanol recovery affirms the potential of this novel pretreatment method as an enhanced form of biofuel production.

*Key words:* bioethanol, lignocellulosic biomass, microwave irradiation, pretreatment, ultrasonication

**Table of Contents**

**Microwave Irradiation with Submerged Ultrasonication: A Novel Lignocellulosic Pretreatment Method**

Fossil fuel dependency and its resulting carbon dioxide emissions is one of the greatest contributors to anthropogenic climate change. As of today, only 23.7% of the global energy reserve is derived from renewable sources (Hussain et al., 2017). In addition, the world population is projected to reach 9.7 billion by 2050, corresponding to a net increase in energy demand by nearly 161 quadrillion British Thermal Units (BTU) (Baruah et al., 2018). With fossil fuel reserves expected to deplete by 2050, discovering an innovative and renewable source of energy that is both environmentally and economically sustainable is a necessity (Aftab et al., 2019).

One promising energy source that is both carbon-neutral and cost-efficient is biomass. In the United States of America (USA), the majority of biofuel is produced from *Zea mays* (corn) and *Saccharum officinarum* (sugarcane) (Journal of Visualized Experiments [JoVE], n.d.). However, they are energy-intensive to grow, fertilizer-dependent, and readily used in other commercial and industrial settings (JoVE, n.d.). Consequently, researchers are looking for other plant-based materials that have the potential to produce energy just as efficiently. Many are currently focusing on grasses, leaves, and crop residues, collectively known as lignocellulosic biomass (LCB).

Being a second-generation feedstock (i.e., non-food material) gives LCB an immediate advantage over conventional sources of bioethanol production. Amounting to a global yield of about 1.3 billion tons per year, LCB is the most abundant bioresource across the globe, yet the majority of it unfortunately remains unutilized (Baruah et al., 2018). If the energy from LCB was harnessed each year, the global bioethanol production would increase by a factor of sixteen, equivalent to 193.6 Ggal of ethanol (Agu et al., 2018; Arora et al., 2020). This is an enormous source of energy that is, for the most part, going to waste.

Unfortunately, the recalcitrant structure of LCB disrupts industrial processes that aim to effectuate bioethanol production, thereby preventing its widespread use. This project aims to investigate a novel pretreatment method that increases the bioethanol recovery from LCB to optimize its potential for use on an industrial scale.

## Background

### *Lignocellulosic Biomass*

The cell wall of LCB is composed of three rigid polymers bonded to one another by hydrogen and Van der Waals bonds: 40–50% cellulose $(C_6H_{10}O_5)_n$, 25–35% hemicellulose $(C_5H_8O_4)_m$, and 15–20% lignin

$[C_9H_{10}O_3(OCH_3)_{0.9-1.7}]_x$, along with small amounts of protein and pectin (Akhtar et al., 2016; Arora et al., 2020; Sun et al., 2016). Cellulose is the primary molecule used for the production of ethanol (Agu et al., 2018). It is a linear polysaccharide consisting of D-glucose subunits bonded to one another by β-1,4-glycosidic linkages and intermolecular hydrogen bonds (Celignis Biomass Analysis Laboratory, n.d.-b; Kumar & Sharma, 2017). Unlike cellulose, hemicellulose is a branched heteropolysaccharide consisting of short chains of xylan, galactomannan, glucuronoxylan, arabinoxylan, and xyloglucan held together by β-1,4- and/or β-1,3-glycosidic bonds (Agu et al., 2018; Zhou et al., 2017). Lignin acts as an adhesion agent by covalently linking cellulose and hemicellulose together (Baruah et al., 2018). Lignin also solidifies the cell structure by the strong entanglement of its three basic subunits: *p*-Coumaryl alcohol, coniferyl alcohol, and sinapyl alcohol (Xu & Ferdosian, 2017; Celignis Biomass Analysis Laboratory, n.d.-b). Unfortunately, lignin amplifies the recalcitrance of LCB, thereby reducing the efficacy of enzymatic hydrolysis (Celignis Biomass Analysis Laboratory, n.d.-b). A simplified breakdown of the molecular structure of LCB can be observed in Figure 1.

**Figure 1**

*Schematic Structure of Lignocellulosic Biomass*

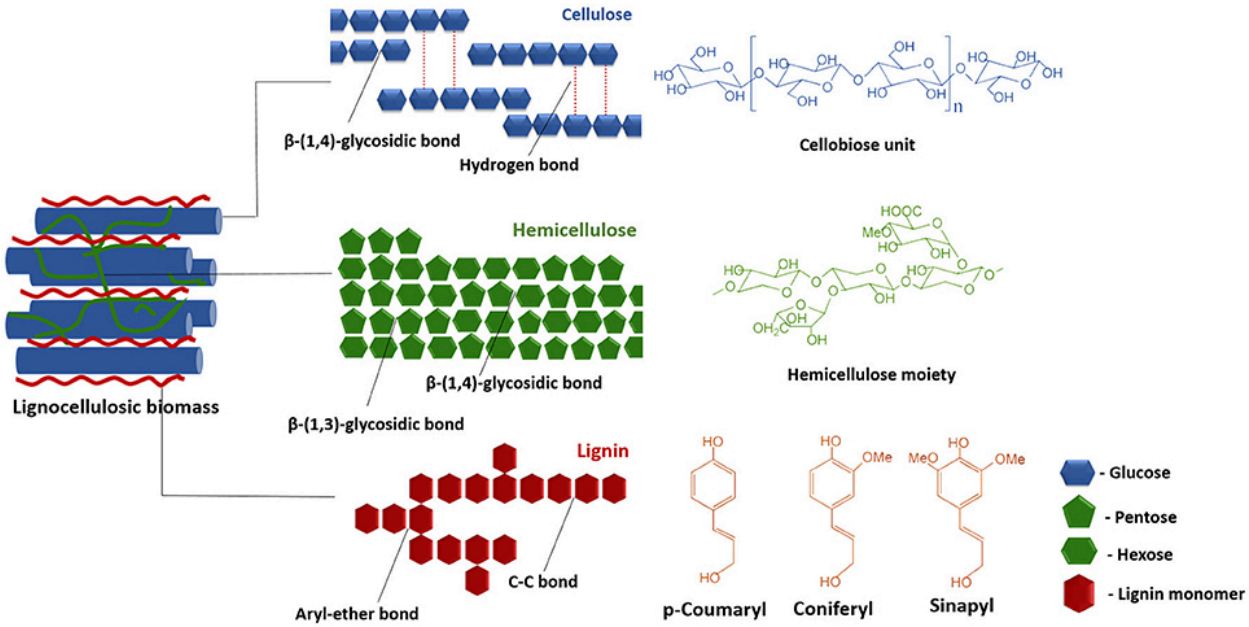

*Note*. From "Recent Trends in the Pretreatment of Lignocellulosic Biomass for Value-Added Products," by J. Baruah, B. K. Nath, R. Sharma, S. Kumar, R. Chandra, D. C. Baruah, & E. Kalita, 2018, *Frontiers in Energy Research* (https://www.frontiersin.org/articles/10.3389/fenrg.2018.00141/full). CC BY-NC.

Of the three polymers composing LCB, cellulose is the primary source of fermentable sugars, namely glucose (JoVE, n.d.). For cellulose to depolymerize at its greatest capacity, it must first be separated from the hemicellulose and lignin components (JoVE, n.d.). Softwoods possess the highest lignin matter, followed by hardwood and then agricultural residues like grasses and stems (Den et al., 2018). It is, therefore, most practical to apply the digestion process to these sources of LCB in order to maximize energy conversion.

Corrugated fibreboard (i.e., one of the most common types of cardboard), shows promise as a sustainable source of biomass for use on the industrial scale. Unlike first-generation feedstocks, it does not require fertilizer maintenance, is not energy-intensive to grow, and does not have competing applications in the food industry. Corrugated fibreboard is also widely abundant as a waste product. In the USA, for example, approximately 80% of all products sold are packaged in corrugated fibreboard (Cardboard Balers, 2017). Consequently, 850 million tons of cardboard and paper are trashed annually, constituting 41% of solid waste in the USA (Cardboard Balers, 2017). The use of corrugated fibreboard for bioethanol production could consume this discarded waste paper to avoid unnecessary utilization of essential first-generation feedstocks. In addition, the conversion of corrugated fibreboard to bioethanol was determined to be the cheapest among all types of waste papers, including newspaper, office paper, and magazines (Wang et al., 2012). The study went on to suggest that bioethanol production from waste papers, especially corrugated fibreboard, is indeed profitable from both technical and economic points of view (Wang et al., 2012).

In addition, corrugated fibreboard has particularly distinguished itself as a superior source of bioethanol over most other lignocellulosic materials (JoVE, n.d.). In fact, in a study that compared the bioethanol recovery of virgin pulp and corrugated fibreboard in sludge form, corrugated fibreboard yielded 11.3% more ethanol than virgin pulp (Boshoff et al., 2015). The team of researchers believe that the lower viscosity of corrugated fibreboard in sludge form resulted in its superior bioethanol recovery. Corrugated fibreboard can, therefore, be used as an easily-accessible proxy for commercially-used biomass.

***Lignocellulosic Pretreatment***

The production of ethanol from LCB is categorized into four primary steps: pretreatment, enzymatic hydrolysis, alcoholic fermentation, and ethanol recovery (Luzzi et al., 2017). The enzymatic hydrolysis of LCB is most efficient when the biomass is first pretreated by chemical, physical, biological, or physicochemical means (Aftab et al., 2019). Breaking down the intermolecular bonds that hold together LCB increases the activity of cellulase enzymes, thereby catalyzing the rate of hydrolysis by three- to ten-fold (Aftab et al., 2019).

The primary goal of pretreatment is to increase the digestibility of carbohydrates with minimal loss of constituent polymers, all while maintaining cost-efficiency and environmental sustainability (Arora et al., 2020). In order to achieve efficient fractionation of LCB, the recalcitrant structure must be disrupted by breaking the lignin sheath, degrading the hemicellulose, and reducing the crystallinity of cellulose (Loow et al., 2015; Chen et al., 2017). As seen in Figure 2, it is equally important to increase the accessibility of the substrate to cellulolytic enzymes by reducing the particle size of LCB, thereby increasing the efficiency of subsequent depolymerization (Den et al., 2018).

**Figure 2**

*Goal of Lignocellulosic Pretreatment Methods*

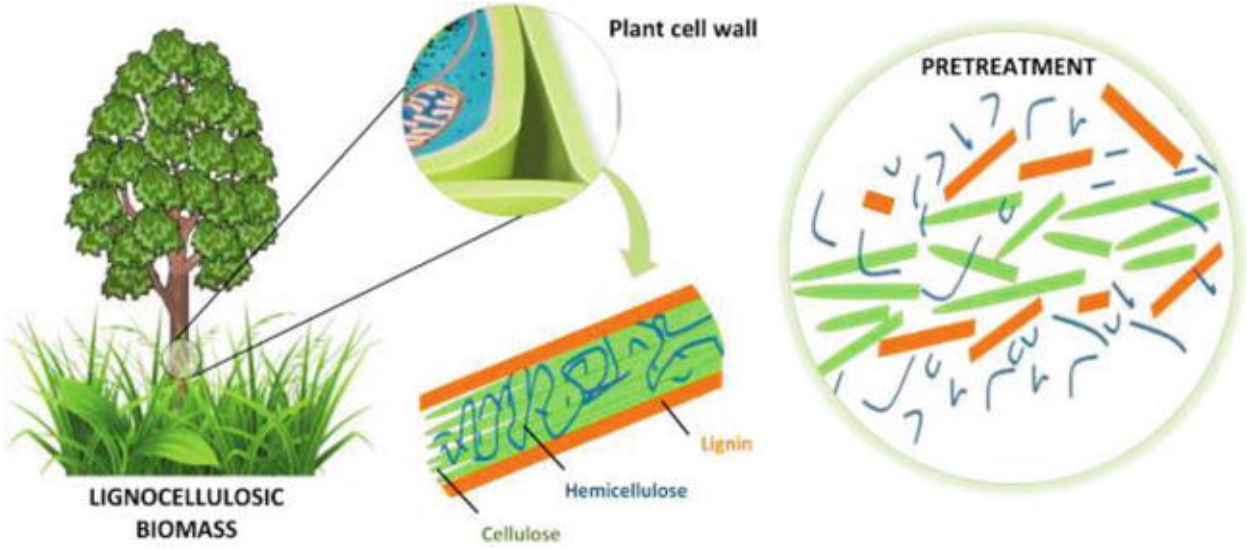


*Note*. Reprinted from *Biomass Fractionation Technologies for a Lignocellulosic Feedstock Based Refinery*, by S. I. Mussatto & G. M. Dragone, 2016, Elsevier Inc. Copyright 2016 by Elsevier Inc.

Although pretreatment is vitally important in the production process, caution must be taken when determining the duration of the pretreatment process. For example, excessive decomposition of LCB can lead to the synthesis of fermentation inhibitors, namely furfural and hydroxymethylfurfural (Den et al., 2018). Scientists, therefore, routinely test novel pretreatment methods over an extensive variety of time periods. Pretreatment of LCB presents several other challenges as well, including high costs, low efficiency, and environmental sustainability. In fact, the energy consumption required for pretreatment has often been higher than the theoretical energy content available in LCB (Kuna et al., 2017). Exploring cheaper and greener pretreatment processes for depolymerizing LCB has, therefore, become a critical subject of study in recent years (Den et al., 2018).

Currently, the most popular pretreatment method incorporates physical and chemical intervention, such as microwave alkali treatment and ultrasonic alkali treatment (Khajavi et al., 2013; Ni et al., 2014; Peng et al., 2013). Although progress has been made, these methods still require large quantities of chemicals and long processing durations of 12–16 h (Gurgel et al., 2008; Hokkanen et al., 2013). It is, therefore, important to explore novel pretreatment methods that are less time- and cost-intensive. Investigating the coupled effects of microwave and ultrasonic irradiation on milled LCB shows promise.

***Innovative Pretreatment Methods***

Milled LCB refers to biomass that has undergone particle size reduction to as little as 0.2 millimetres in the interest of reducing molecular crystallinity (Aftab et al., 2019; Baruah et al., 2018). In doing so, a considerable increase in surface area is achieved, thereby rendering LCB more amenable to cellulases during enzymatic hydrolysis (Aftab et al., 2019). Milling LCB is an effective preliminary pretreatment method since it does not produce any toxic or inhibitory compounds as is the case with chemical intervention (Baruah et al., 2018).

The use of microwave (MW) irradiation as a pretreatment method for LCB has recently been popularized. This technology presents several advantages that make the pretreatment process more environmentally and economically sustainable. MW irradiation refers to electromagnetic waves consisting of both electric and magnetic fields within the frequency band of 300 MHz and 300 GHz (Agu et al., 2018). A domestic MW oven operates at a frequency of 2,450 MHz ($\lambda$ = 12.24 cm) which is a commonly used value for LCB pretreatment (Agu et al., 2018; Aftab et al., 2019).

When an oscillating MW electromagnetic field interacts with polarizable molecules or ions, such as in LCB,

rapid heating occurs as the polarized species fight to align with the field (Ritter, 2014). The friction provoked by the rotation and collisions of the molecules creates enough heat to break the molecular bonds of LCB (Ritter, 2014). Substrate availability increases as a result, thereby fulfilling the primary goal of pretreatment (Aftab et al., 2019).

Employing MW irradiation as a LCB pretreatment method poses numerous advantages, the greatest being a ten-fold reduction in processing time compared to using other forms of electromagnetic radiation (Agu et al., 2018). Other advantages include controlled heating (i.e., having an instantaneous on-off operation), increased heating capacity, quicker heat transference, low inhibitor formation, among others (Agu et al., 2018; Aftab et al., 2019). One major disadvantage of MW irradiation is its inability to effectively penetrate bulk materials. Milling LCB is, therefore, an essential preceding step that prevents temperature gradients from forming within the samples that would otherwise diminish the pretreatment process (Aftab et al., 2019; Agu et al., 2018). MW irradiation is also known to degrade glucose into hydroxymethylfurfural if the effects exceed a critical point (McParland et al., 2003).

Despite its few disadvantages, MW irradiation has been proven to disrupt the complex fibre structure of LCB by removing a significant proportion of hemicellulose, resulting in a recovery of up to 93.05% of cellulose (Liu et al., 2018). Cellulose that is more accessible to enzymes leads to a greater yield of free glucose following enzymatic hydrolysis (Agu et al., 2018). In recent years, pretreating LCB with MW irradiation, especially in combination with other pretreatment methods, has been an area of great interest (Baruah et al., 2018). Many facets of this technology are yet to be explored, such as combining MW irradiation with other physical methods.

Ultrasonic (US) irradiation is another relatively-new pretreatment technique for fracturing the rigid structure of LCB. Ultrasonication has different effects on the pretreatment of LCB largely depending on three variables: frequency, power, and duration (Baruah et al., 2018). In any case, ultrasounds rely on the principle of cavitation to form empty grooves which extract hemicellulose and lignin from LCB in the interest of facilitating subsequent hydrolysis (Ravichandran & Jaiswal, 2016). The effects of US irradiation could be amplified if LCB is submerged since sound travels five times faster underwater than in air (Ulin, 2011).

US irradiation increases substrate availability which allows for quicker depolymerization of the polysaccharides in LCB (Luzzi et al., 2017). In fact, using ultrasonication as a pretreatment method for LCB can reduce the hydrolysis time by up to 80% (Baruah et al., 2018). Unfortunately, US irradiation can form inhibitors that deactivate important enzymes depending on the chosen values for frequency, power, and duration (Luzzi et al.,

2017). It is, therefore, essential to experiment with a wide range of US intensities in order to determine the optimal settings for industrial use. Many researchers are currently exploring the effects of 40 kHz on LCB degradation (Cherpozat et al., 2017; Ivetic et al., 2017). Due to the novelty of US irradiation, this technology remains vastly unexplored, especially in combination with other pretreatment methods.

***Enzymatic Hydrolysis***

Following pretreatment, enzymatic hydrolysis is the second step in the process of converting LCB to bioethanol. This step must proceed pretreatment because unfractured lignin naturally reduces hydrolysis reactions by blocking substrates from hydrolyzing (Agu et al., 2018). Once pretreatment has successfully compromised the blocking ability of lignin, the β-1,4-glycosidic linkages can be severed to break down the cellulose into glucose subunits (Den et al., 2018). Breaking the intermolecular hydrogen bonds that exist between unbranched cellulose chains is equally important (Den et al., 2018). Only then is LCB prepared for subsequent fermentation.

During the saccharification process, three primary types of cellulase enzymes are employed, often in a 1% w/v concentration (Wang et al., 2020). The first type is endocellulase which works to produce oligosaccharides of varying lengths by hydrolyzing β-1,4-glycosidic linkages at random (Agu et al., 2018). The second type is exocellulase, also called cellobiohydrolase, which hydrolyzes cellulose chains on both ends, releasing cellobiose in the process (Agu et al., 2018). Lastly, β-glucoside glucohydrolase, better known as β-glucosidase, hydrolyzes the remaining cellodextrins to form glucose (Agu et al., 2018). Figure 3 displays a breakdown of this enzyme cascade.

**Figure 3**

*Schematic Flowchart of Cellulase Enzyme Cascade*

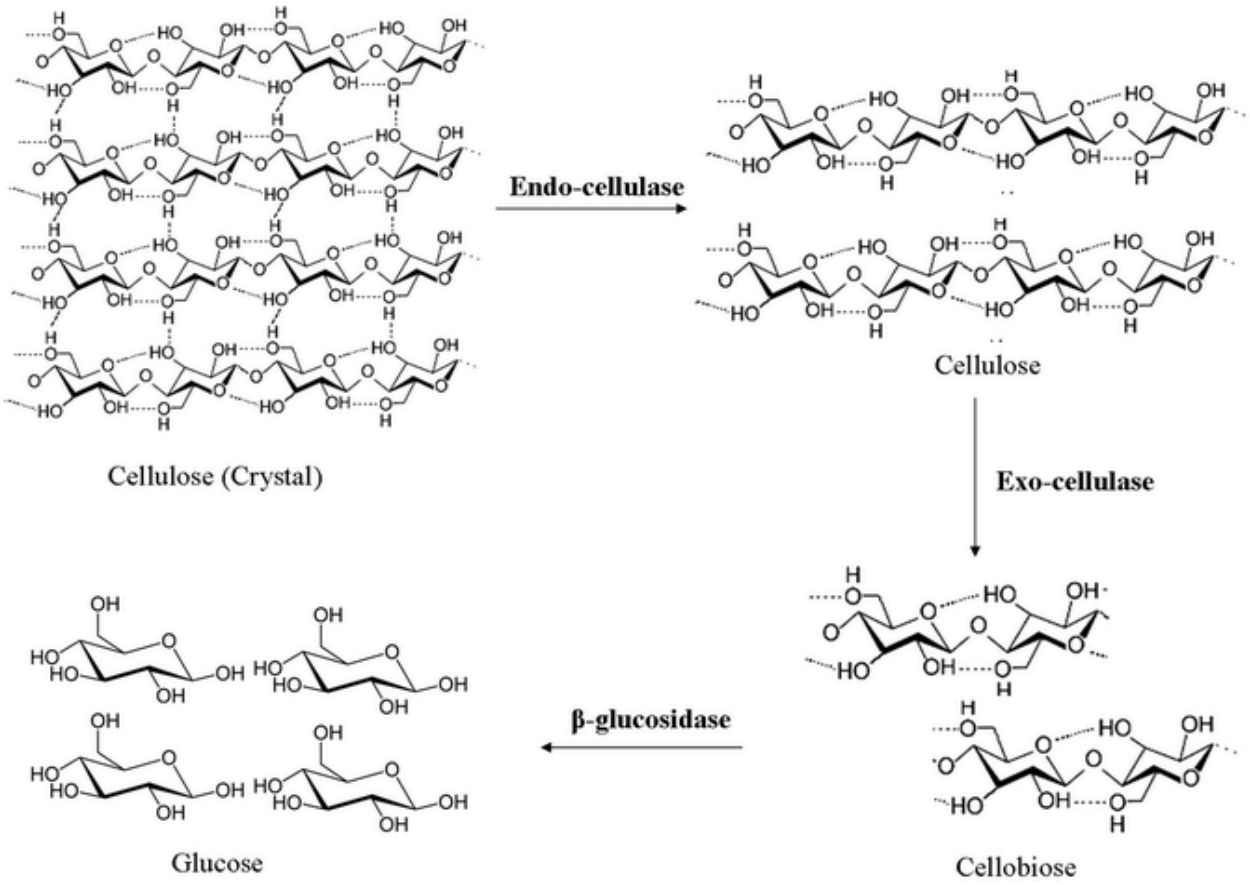


*Note*. Reprinted from *Biotechnology for Environmental Management and Resource Recovery*, by R. Gupta, G. Mehta, D. Deswal, S. Sharma, K. K. Jain, R. C. Kuhad, & A. Singh, 2013, Springer. Copyright 2013 by Springer.

While depolymerizing hemicellulose is not necessary for bioethanol production, endo-β-1,4-xylanase is the best enzyme for hydrolyzing its constituent polymers (Agu et al., 2018). All cellulases and hemicellulases work best at a temperature between 40–50 ℃ for about 24 h (Agu et al., 2018; JoVE, n.d.).

***Alcoholic Fermentation and Ethanol Recovery***

In the third step of LCB biofuel production, glucose is fermented with yeast to produce bioethanol (JoVE, n.d.). While saccharification operates best at high temperatures, alcoholic fermentation is optimized at approximately 37 ℃ (Azhar et al., 2017). It is imperative that fermentation proceeds enzymatic hydrolysis because yeast is unable to ferment polysaccharides (Celignis Biomass Analysis Laboratory, n.d.-a).

*Saccharomyces cerevisiae* (*S. cerevisiae*) and its recombinant forms have continuously proven to be superior fermentation agents for ethanol production. *S. cerevisiae* is the common nutritional yeast sold at many

grocery stores and is known to have a variety of applications (Kerns, n.d.). In the context of biofuel production, *S. cerevisiae* plays a very important role in converting glucose to ethanol. In both aerobic and anaerobic conditions, glucose is naturally converted into pyruvate during glycolysis (Dashko et al., 2014). The pyruvate molecule subsequently loses a carboxyl group, yielding acetaldehyde and releasing carbon dioxide in the process (Dashko et al., 2014). Reduced nicotinamide adenine dinucleotide (NADH) reduces acetaldehyde to form ethanol with NAD+ as a by-product. (Dashko et al., 2014). Since the gas above a liquid contains about the same concentration of ethanol as the liquid itself, the resulting concentration can be quantified using an ethanol sensor to analyze the efficacy of the chosen production method.

***Industrial Potential***

Although MW and US irradiation have individually gained research attention in recent years, there is still more to be discovered regarding their effects on LCB (Agu et al., 2018). The current methods for pretreating LCB on an industrial scale are too costly compared to conventional biofuel production methods. Microwaves and ultrasounds, however, are efficient and reusable. The induction of these technologies for industrial use, therefore, has the potential to reduce the cost of producing bioethanol from LCB (Agu et al., 2018). It would be interesting to identify whether a synergistic relationship exists between these pretreatment methods. For example, exposing biomass to MW irradiation first could allow for better isolation of cellulose during ultrasonication by reducing the length of the filaments in the hemicellulose-lignin matrix. Based on a thorough literature review of the individual effects of MW and US irradiation on the delignification of LCB, the combination of these pretreatment methods has the potential to enhance current biofuel production techniques.

**Purpose**

To determine the microwave power (W) and duration of submerged ultrasonication (s) that, when applied together, result in the greatest bioethanol recovery from corrugated fibreboard in the interest of alleviating the environmental and economic burdens of current pretreatment methods for LCB and, thereby, optimizing its potential as a renewable source of energy.

**Hypothesis**

In the research plan, it was originally believed that the greatest bioethanol recovery would result from a MW power of 1,100 W and a duration of submerged ultrasonication of 480 s. Upon further review of published

literature, it is now believed that at 180 W of MW power and 420 s of submerged ultrasonication, the greatest bioethanol recovery from corrugated fibreboard will be achieved. The synergistic effect of these selected values for MW and US irradiation is believed to result in the greatest disruption of the recalcitrant structure of LCB to allow for better enzyme accessibility during subsequent hydrolysis.

When LCB is exposed to MW irradiation, the rising temperature of the biomass breaks the bonds connecting the glucose subunits together. If the effect of MW irradiation is too high, however, glucose degrades into hydroxymethylfurfural (McParland et al., 2003). Studies have reported that a MW power of 180 W allows for the greatest fractionation of LCB with minimal volumetric loss due to heat-induced evaporation and/or glucose degradation (Saifuddin et al., 2013).

Since the use of US irradiation in lignocellulosic pretreatment is relatively unexplored, published studies regarding its application on corrugated fibreboard are scarce. Since the molecular composition of corrugated fibreboard and wheat straw are close to identical, their chemical behaviour is nearly the same (del Río et al., 2012; Ma et al., 2015). In a study that investigated the effects of the duration of ultrasonication on the delignification of wheat straw, it was found that a US irradiation time of 35 min was optimal (Sun & Tomkinson, 2002). Since sound travels five times faster underwater than in air, the hypothesized optimal duration of submerged ultrasonication for this experiment is 7 min, or 420 s (Ulin, 2011). In combination with the selected MW power setting above, it is believed that the resulting digestibility of corrugated fibreboard will optimize its potential for industrial use.

## Methodology

### Variables

For this experiment, there are two independent variables: MW power (W) and duration of submerged ultrasonication (s). This experiment hopes to elucidate the synergistic effect of these two existing pretreatment methods on the digestibility of cellulose in corrugated fibreboard, a prominent source of LCB, for subsequent saccharification and fermentation. The dependent variable in this experiment is the resulting bioethanol concentration (% v/v).

To ensure maximal accuracy, several other variables will be controlled. Firstly, all samples will come from the same sheet of corrugated fibreboard. They will be milled by the same food processor at the same power setting for a total duration of 15 min. Additionally, all samples will begin with the same amount of store-bought

steam-distilled, ozonated water (35 mL). Furthermore, the duration and frequency of the MW irradiation will be held constant at 8 min and 2,450 MHz, respectively. Also, the frequency and power of the submerged ultrasonication will also be held constant at 42 kHz and 35.00 W, respectively. The water temperature of the ultrasonic bath will also be controlled at 20.4 °C. In addition, the same amount of cellulase (i.e., 0.35 g) and active yeast for traditional baking (i.e., 5.3 g) will be added to each of the samples. Between each day of the experiment, the samples will be placed in an incubator for 24 h at a temperature of 40 °C.

Additionally, there will be a control group for this experiment to test the significance of the independent variables. The control group will be milled, but will not be pretreated with MW or US irradiation. Instead, it will proceed directly to enzymatic hydrolysis. In addition, there will be samples that undergo MW irradiation but not ultrasonication, and vice versa. This will ensure a maximal understanding of the relationship between microwaves and ultrasounds on the pretreatment of corrugated fibreboard.

**Materials**

***Appliances***

1 Braun Multimix food processor (1 head and 1 base); 1 Corning PC–420 Laboratory Stirrer; 1 Lab-Line's Low Cost Gravity Convection Oven incubator; 1 MAGNASONIC Digital Ultrasonic Jewelry Cleaner; and 1 Maytag MMV5207ACS microwave oven.

***Clean-Up***

1 compost bin; 1 garbage bin; 1 recycling bin; 1 waste disposal bin; and 225 sheets of paper towel.

***Glassware***

1 10-mL graduated cylinder (TC 20 °C, ±0.2 mL); 1 250-mL graduated cylinder (TC 20 °C, ±2 mL); 1 500-mL beaker (±5%); 1 500-mL graduated cylinder (TC 20 °C, ±5 mL); 2 100-mL graduated cylinder (TC 20 °C, ±1 mL); 12 30-mL glass vials; and 14 250-mL Erlenmeyer flasks (±5%).

***Measuring Instruments***

1 30-cm analog ruler to the nearest millimetre; 1 analog thermometer to the nearest degree Celsius; 1 PASPORT Ethanol Sensor (1 probe and 1 amplifier, ±2.1% (experimentally-determined)); and 1 Scout Pro SPE402 digital electronic balance to the nearest hundredth of a gram.

***Miscellaneous***

1 19 cm x 19 cm corkboard; 1 iPhone 8 Plus; 1 roll of masking tape; 1 Sharpie permanent marker; and 72 sheets of weighing paper.

***Safety Equipment***

1 dry-chemical fire extinguisher; 2 pairs of eye goggles; and 18 pairs of nitrile powder-free gloves.

***Substances***

6.67 mL of 100% v/v solution of ethanol; 3 15 cm x 20 cm x 0.4 cm sheets of corrugated fibreboard; 12.6 g of powdered cellulase; 190.8 g of active dry yeast for traditional baking (*S. cerevisiae*); 1,920 mL of tap water; and 5,208.33 mL of steam-distilled, ozonated water.

***Tools***

1 250-mL wash bottle; 1 magnetic rod; 1 scoopula; 1 SPARK Science Learning System; 1 stir bar magnet; 1 strainer; 1 test tube holder; 1 X-ACTO® knife; 12 airlocks; and 14 Erlenmeyer flask stoppers.

**Procedure**

The experimental procedure consists of three phases: pretreatment and enzymatic hydrolysis; alcoholic fermentation; and ethanol detection. The three phases of the method will be repeated three times to cover all possible combinations of selected values for the independent variables. The camera of an iPhone 8 Plus will be used to photograph the progress of the experiment; these photographs will be documented in Appendix B. During the first phase, the samples will be milled using a food processor and subsequently pretreated with MW and US irradiation of varying amounts. Afterwards, the pretreated samples will be treated with cellulase and left to incubate for a period of 24 h. During the second phase of the experiment, each sample will be mixed with a proportional amount of active yeast for traditional baking (*S. cerevisiae*) to induce alcoholic fermentation. After a second incubation period of 24 h, the third phase will begin and consist of quantifying the bioethanol concentration of each sample using a PASPORT Ethanol Sensor calibrated to a 1% v/v solution of ethanol. A step-by-step experimental procedure is detailed below.

***Day 1: Pretreatment and Enzymatic Hydrolysis***

(1) Put on a pair of nitrile powder-free gloves; (2) put on a pair of eye goggles; (3) place the dry-chemical fire extinguisher within about a 5-metre radius of the workstation; (4) fill the 250-mL wash bottle with

steam-distilled, ozonated water; (5) zero the Scout Pro SPE402 digital electronic balance; (6) place the base of the Braun Multimix food processor on the electronic balance and record the mass; (7) cut the 15 cm x 20 cm x 0.4 cm sheet of corrugated fibreboard into 75 2 cm x 2 cm x 0.4 cm square prisms using the X-ACTO® knife and the 30-cm analog ruler; (8) fill the 500-mL beaker with 300 mL of steam-distilled, ozonated water; (9) fully submerge all 75 square prisms of corrugated fibreboard in the beaker for approximately 30 s; (10) pour the contents of the beaker through a strainer to collect the drenched square prisms of corrugated fibreboard; (11) place all 75 of the drenched square prisms inside the base of the food processor; (12) secure the head of the food processor onto its base and process the materials on the highest power setting for 10 min; (13) measure 250 mL of steam-distilled, ozonated water using the 250-mL graduated cylinder; (14) pour the water into the food processor and process the materials on the highest power setting for an additional 5 min; (15) zero the electronic balance; (16) place the base of the food processor with the materials inside on the electronic balance and record the mass; (17) after clearing the electronic balance of any materials, remove the lid from one of the 30-mL glass vials and place it on the balance; (18) zero the electronic balance; (19) use a scoopula to transfer milled corrugated fibreboard into the glass vial until the electronic balance reads 17.00 g; (20) place the glass vial into the Maytag MMV5207ACS microwave oven; (21) repeat steps 17–20 using 5 additional glass vials; (22) microwave the 6 glass vials for 8 min at 100% power (1,100 W); (23) remove the 6 glass vials from the microwave oven using the test tube holder and place them on the 19 cm x 19 cm corkboard; (24) after a cooling period of about 2 min, carefully screw the lid back onto each of the glass vials; (25) measure 400 mL of tap water using a 500-mL graduated cylinder; (26) pour the tap water into the tank of the MAGNASONIC Digital Ultrasonic Jewelry Cleaner; (27) place one of the glass vials into the tank of the sonicator; (28) turn the sonicator on and leave the glass vial inside for a set duration of 480 s; (29) remove the glass vial from the sonicator and dry it with 1 sheet of paper towel; (30) unscrew the lid from the glass vial and pour the contents from inside into one of the 250-mL Erlenmeyer flasks; (31) measure 10 mL of steam-distilled, ozonated water using the 10-mL graduated cylinder; (32) pour the water into the glass vial and screw the lid back on; (33) shake the glass vial for about 10 s; (34) unscrew the lid from the glass vial and pour the contents from inside into the same Erlenmeyer flask; (35) swirl the Erlenmeyer flask to mix the contents for approximately 30 s; (36) repeat steps 31–35 one more time; (37) label the Erlenmeyer flask with its respective parameters using a small piece of masking tape and a Sharpie permanent marker; (38) repeat steps 27–37 five more times using the other set durations of

submerged ultrasonication during step 28 (380 s, 280 s, 180 s, 90 s, and 0 s); (39) repeat steps 17–38 one more time using the other set power setting of MW irradiation during step 22 (80% [880 W]); (40) pour the tank water of the sonicator down the sink and dry the interior using 1 sheet of paper towel; (41) using the wash bottle and 9 sheets of paper towel, rinse and dry the food processor, the scoopula, and the 12 glass vials; (42) set the Lab-Line's Low Cost Gravity Convection Oven (incubator) to 40 °C and place a thermometer inside; (43) place a sheet of weighing paper on the electronic balance; (44) zero the electronic balance; (45) use a scoopula to transfer powdered cellulase onto the balance until it reads 0.35 g; (46) carefully pour the cellulase from the weighing paper into one of the Erlenmeyer flasks; (47) dispose of the weighing paper in the recycling bin; (48) place the Erlenmeyer flask on the Corning PC–420 Laboratory Stirrer; (49) after placing a stir bar magnet inside the Erlenmeyer flask, electronically stir the contents of the flask on the highest power setting for 5 min; (50) remove the stir bar magnet from the flask using a magnetic rod; (51) place a stopper on the Erlenmeyer flask; (52) using the wash bottle and 1 sheet of paper towel, rinse and dry the stir bar magnet and magnetic rod; (53) repeat steps 43–52 for the other 11 Erlenmeyer flasks; (54) once the thermometer inside the incubator reads 40 °C, place all of the Erlenmeyer flasks inside; (55) compost the 34 sheets of paper towel; (56) dispose of the gloves in the garbage; and (57) begin *Day 2: Alcoholic Fermentation* in 24 h.

***Day 2: Alcoholic Fermentation***

(1) Put on a pair of nitrile powder-free gloves; (2) put on a pair of eye goggles; (3) fill the 250-mL wash bottle with steam-distilled, ozonated water; (4) remove all 12 Erlenmeyer flasks from the incubator; (5) place a sheet of weighing paper on the electronic balance; (6) zero the electronic balance; (7) use a scoopula to transfer active yeast for traditional baking (*S. cerevisiae*) onto the balance until it reads 5.3 g; (8) remove the stopper from one of the Erlenmeyer flasks; (9) carefully pour the active dry yeast from the weighing paper into the Erlenmeyer flask; (10) dispose of the weighing paper in the recycling bin; (11) place the Erlenmeyer flask on the Corning PC–420 Laboratory Stirrer; (12) after placing a stir bar magnet inside the Erlenmeyer flask, electronically stir the contents of the flask on the highest power setting for 5 min; (13) remove the stir bar magnet from the flask using a magnetic rod; (14) fill one of the airlocks with tap water up to the indicated line (about 20 mL); (15) place the airlock on top of the Erlenmeyer flask and secure it to the flask with masking tape; (16) using the wash bottle and 1 sheet of paper towel, rinse and dry the stir bar magnet and magnetic rod; (17) repeat steps 5–16 for the other 11

Erlenmeyer flasks; (18) adjust the incubator setting if necessary to ensure that the thermometer still reads 40 ℃; (19) place all of the Erlenmeyer flasks inside; (20) compost the 12 sheets of paper towel; (21) dispose of the gloves in the garbage; and (22) begin *Day 3: Ethanol Detection* in 24 h.

***Day 3: Ethanol Detection***

(1) Put on a pair of nitrile powder-free gloves; (2) put on a pair of eye goggles; (3) open a nearby window for continuous ventilation; (4) fill the 250-mL wash bottle with steam-distilled, ozonated water; (5) remove all 12 Erlenmeyer flasks from the incubator and let them cool down for about 1 h to reach room temperature; (6) measure 0.35 mL of a 100% v/v solution of ethanol using a 10-mL graduated cylinder; (7) pour the ethanol into a different 250-mL Erlenmeyer flask; (8) measure 34.65 mL of steam-distilled, ozonated water using a 100-mL graduated cylinder; (9) pour the steam-distilled, ozonated water into the Erlenmeyer flask; (10) place a stopper on the Erlenmeyer flask; (11) swirl the Erlenmeyer flask for about 30 s to mix thoroughly; (12) label the Erlenmeyer flask with *35 mL of 1% v/v ethanol solution* using a small piece of masking tape and a Sharpie permanent marker; (13) connect the probe of the PASPORT Ethanol Sensor to the amplifier; (14) connect the amplifier to the SPARK Science Learning System; (15) once the sensor is fully assembled and turned on, wait about 10 min for the temperature of the sensor to stabilize; (16) remove the stopper from the Erlenmeyer flask containing the 1% v/v solution of ethanol; (17) place the probe of the ethanol sensor inside of the Erlenmeyer flask so that the end is 1 cm above the solution; (18) secure the stopper of the probe on the head of the Erlenmeyer flask; (19) press and hold the 1% CAL button on the sensor for 4 s to calibrate the sensor once the ethanol readings on the SPARK Science Learning System have stabilized for at least 30 s; (20) remove the ethanol sensor from the Erlenmeyer flask and place the original stopper back on the flask; (21) repeat steps 6–11 with 0.18 mL of a 100% v/v solution of ethanol and 69.82 mL of steam-distilled, ozonated water; (22) remove the stopper from the Erlenmeyer flask; (23) measure 35 mL of the solution using a different 100-mL graduated cylinder; (24) pour the remaining contents of the Erlenmeyer flask in the waste disposal bin; (25) using the wash bottle and 1 sheet of paper towel, rinse and dry the Erlenmeyer flask; (26) pour the contents of the 100-mL graduated cylinder back into the Erlenmeyer flask; (27) repeat steps 17–18 for this Erlenmeyer flask; (28) at the home screen of the SPARK Science Learning System, record the displayed value of the ethanol concentration once the value has stabilized for at least 30 s; (29) remove the ethanol sensor from the Erlenmeyer flask; (30) repeat steps 24–25 for this Erlenmeyer flask; (31) repeat steps

21–30 seven more times with 0.36 mL, 0.52 mL, 0.70 mL, 0.88 mL, 1.06 mL, 1.22 mL, and 1.40 mL of a 100% v/v solution of ethanol and 69.64 mL, 69.48 mL, 69.30 mL, 69.12 mL, 68.94 mL, 68.78 mL, 68.60 mL of steam-distilled, ozonated water, respectively; (32) remove the airlock and masking tape from one of the Erlenmeyer flasks containing fermented corrugated fibreboard; (33) repeat steps 27–29 for the Erlenmeyer flask; (34) repeat steps 32–33 for the other 11 Erlenmeyer flasks; (35) remove any stoppers from the 13 remaining Erlenmeyer flasks and pour the contents of them in the waste disposal bin; (36) using the wash bottle and 13 sheets of paper towel, rinse and dry the Erlenmeyer flasks; (37) compost the 39 sheets of paper towel; (38) dispose of the gloves in the garbage; and (39) repeat days 1–3 (omitting steps 5–6 and 15–16 of day 1, and steps 6–12 of day 3) twice more using the other set power settings of MW irradiation during step 22 of day 1 (0% [0 W], 20% [220 W], 40% [440 W], 60% [660 W]).

## Results

This experiment determined the concentration of bioethanol produced from corrugated fibreboard that had been subjected to varying strengths of MW irradiation and varying durations of submerged ultrasonication. The power of the MW irradiation was applied at values of 0 W, 220 W, 440 W, 660 W, 880 W, and 1,100 W. The duration of the submerged ultrasonication was set at values of 0 s, 90 s, 180 s, 280 s, 380 s, and 480 s. The combination of these selected values for MW power and duration of submerged ultrasonication resulted in an array of ethanol concentrations (reference Table 2 in Appendix A).

To determine the percent deviation of the observed measurements, a separate study was conducted on known ethanol concentrations in solution. Firstly, the volumes of a 100% v/v ethanol solution and of steam-distilled, ozonated water required to create selected concentrations of ethanol in solution (i.e., 0.25% v/v, 0.50% v/v, 0.75% v/v, 1.00% v/v, 1.50% v/v, 1.75% v/v, and 2.00% v/v) were determined algebraically in Table 5 of the journal. These mixtures were created during the third day of the experimental procedure. The ethanol concentration of each sample as measured by the PASPORT ethanol sensor was 0.26% v/v, 0.50% v/v, 0.72% v/v, 0.99% v/v, 1.28% v/v, 1.47% v/v, 1.71% v/v, and 2.03% v/v, respectively. The mean percent deviation of the samples was determined to be 2.1%. This percent error will be used herein to determine the accuracy range of notable measurements. To confirm this value of uncertainty, the experimental data was plotted against the theoretical values that were calculated, as seen in Figure 4.

**Figure 4**

*Graph 1: Percent Deviation of Ethanol Concentration in Solution*

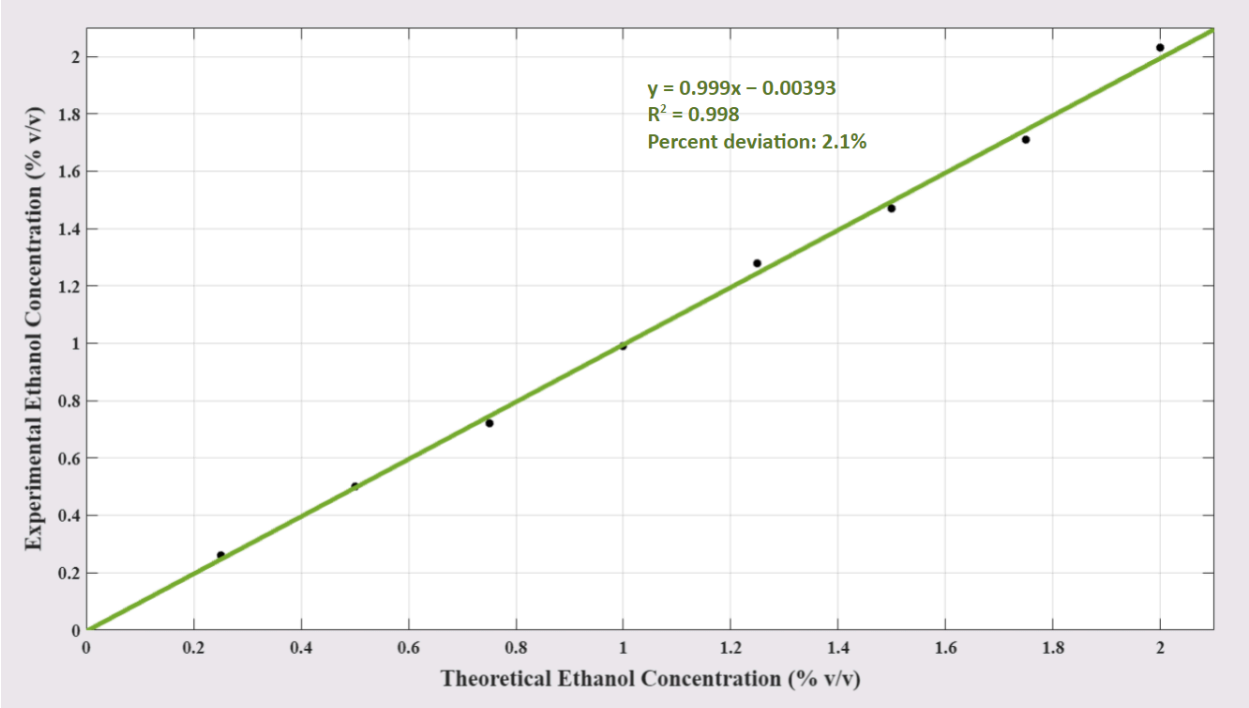


A polynomial equation to the first degree best represents the correlation between the theoretical and experimental ethanol concentrations in solution. This linear equation is represented by the green line in Figure 4 and can be expressed to three significant digits as follows:

$$y = 0.999x - 0.00393. \quad (1)$$

The coefficient of determination for this equation is $R^2 = 0.998$, indicating that the data fits strongly to the regression curve. This strong fit confirms the low value obtained for the percent deviation between theoretical and experimental ethanol concentrations in solution.

Upon determining the percent error of the PASPORT ethanol sensor, the sensor was then used to collect measurements for this experiment. A clear analysis of this quantitative data requires the assignment of names for each of the independent and dependent variables being studied. The variables of this experiment from this point on are defined as follows: x represents the MW power applied to the corrugated fibreboard in watts; y represents the duration of submerged ultrasonication undergone by the corrugated fibreboard in seconds; and f(x) and f(y)

represent the bioethanol concentration in percent derived from the corrugated fibreboard as a function of the MW power and duration of submerged ultrasonication, respectively.

Prior to examining the possible synergistic relationship between MW and US irradiation, it is important to analyze these independent variables individually. Six samples were pretreated with only MW irradiation while six others were pretreated with only US irradiation. For the samples not exposed to US irradiation, MW power was applied at values of 0 W, 220 W, 440 W, 660 W, 880 W, and 1,100 W. Following the conversion process, the ethanol concentrations of these samples were determined to be 1.73% v/v, 1.76% v/v, 1.96% v/v, 1.93% v/v, 1.77% v/v, and 1.74% v/v, respectively. This data was plotted on a two-dimensional Cartesian coordinate system (Figure 5).

**Figure 5**

*Graph 2: Recovered Bioethanol Concentration from Microwaved Corrugated Fibreboard*

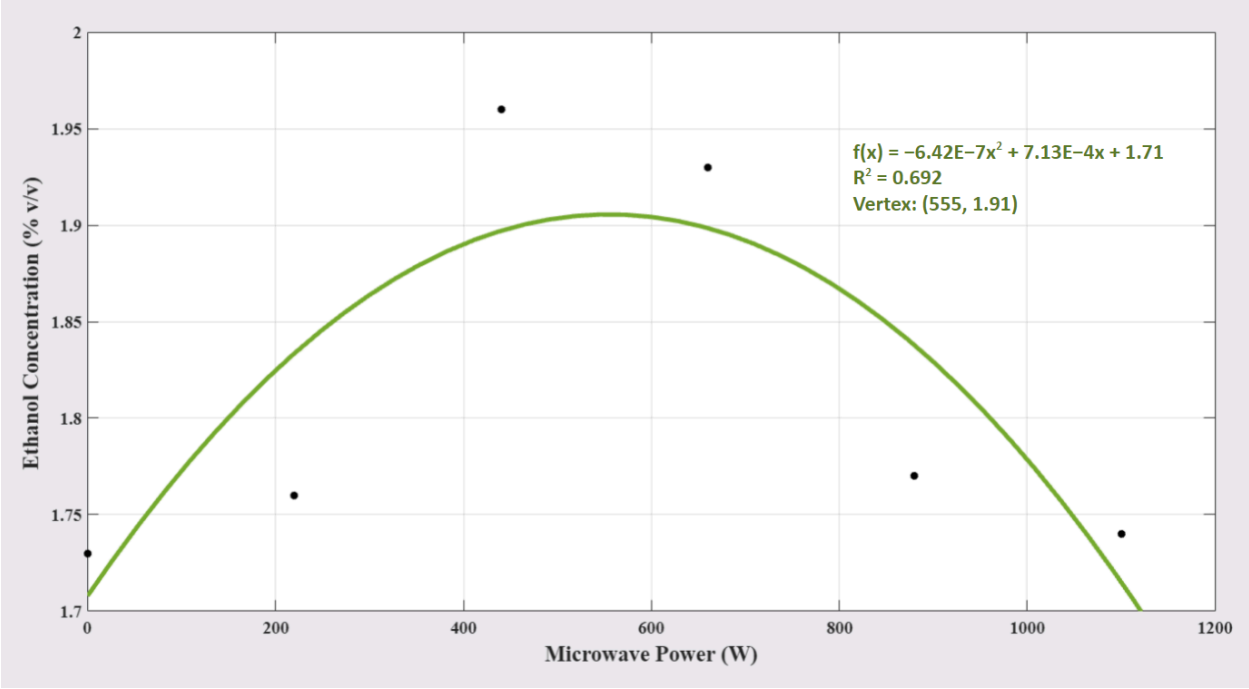


*Note*. The duration and frequency of the MW irradiation was held constant at 8 min and 2,450 MHz, respectively. These samples were not exposed to submerged ultrasonication.

A polynomial equation to the second degree best represents the correlation between MW power and ethanol concentration. This quadratic equation is represented by the green curve in Figure 5 and can be expressed to three significant digits as follows:

$$f(x) = -6.42E{-}7x^2 + 7.13E{-}4x + 1.71. \quad (2)$$

The coefficient of determination for this equation is $R^2 = 0.692$, indicating that the data fits moderately close to the regression curve. The vertex of the parabola, which can be calculated algebraically, was determined to be (555, 1.91). 555 W is, therefore, the optimal power setting for recovering bioethanol from milled corrugated fibreboard that is only pretreated with MW irradiation. On either side of this vertex, the ethanol concentration decreases toward zero, as partially seen on Figure 5. This indicates that too little or too much MW irradiation is damaging to the pretreatment process.

A different set of six samples were tested at varying values of duration of submerged ultrasonication with no MW irradiation. For these samples, US irradiation was applied for durations of 0 s, 90 s, 180 s, 280 s, 380 s, and 480 s. Following the conversion process, the ethanol concentrations of the samples were determined to be 1.73% v/v, 1.77% v/v, 1.79% v/v, 1.87% v/v, 1.85% v/v, and 1.85% v/v, respectively. Similar to above, this data was plotted on a two-dimensional Cartesian coordinate system (Figure 6).

**Figure 6**

*Graph 3: Recovered Bioethanol Concentration from Sonicated Corrugated Fibreboard*

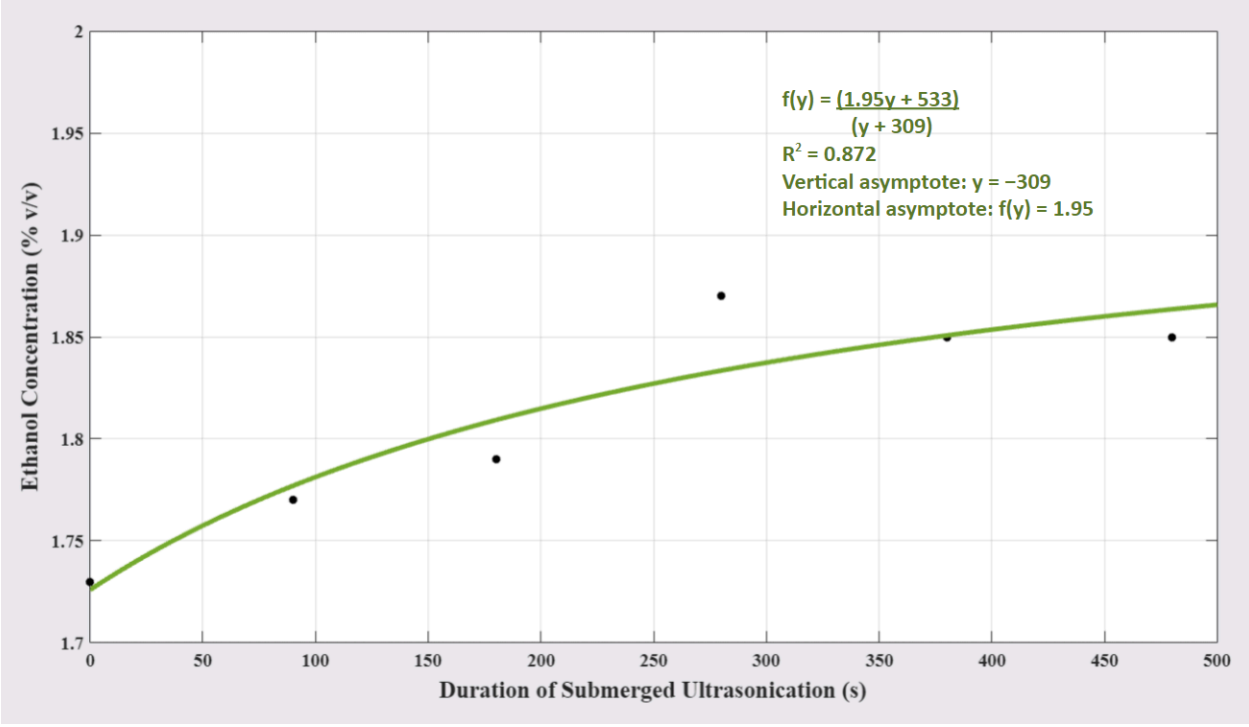

*Note*. The frequency and power of the submerged ultrasonication was held constant at 42 kHz and 35.00 W, respectively. These samples were not exposed to MW irradiation.

A rational equation with polynomials to the first degree in both the numerator and denominator best represents the correlation between duration of submerged ultrasonication and ethanol concentration. This rational equation is represented by the green curve in Figure 6 and can be expressed to three significant digits as follows:

$$f(y) = \frac{(1.95y + 533)}{(y + 309)}. \quad (3)$$

The coefficient of determination for this equation is $R^2 = 0.872$, indicating that the data fits strongly to the regression curve. The vertical and horizontal asymptotes, which can be calculated algebraically, were determined to be y = −309 and f(y) = 1.95, respectively. While the vertical asymptote has little contextual meaning, the horizontal asymptote indicates the value of ethanol concentration that is approached as the duration of submerged ultrasonication approaches positive infinity. In other words, slightly below an ethanol concentration of 1.95% v/v is the highest possible theoretical value that can be obtained from pretreating milled corrugated fibreboard with only US irradiation from the specifications of this experiment. The presence of a horizontal asymptote also indicates that the ethanol concentration increases with duration of submerged ultrasonication with progressively smaller intervals of increase as duration approaches positive infinity, as seen on Figure 6.

Based on the data collected in these semi-controlled groups, the peak bioethanol concentration of pretreating LCB with only ultrasonication theoretically surpasses that of only applying MW irradiation. The combination of these pretreatment methods with MW irradiation preceding submerged ultrasonication, however, yielded even greater results. Using a three-dimensional Cartesian coordinate system with MW power on the x-axis, duration of submerged ultrasonication on the y-axis, and ethanol concentration on the z-axis, the synergistic relationship between these variables can be easily observed. Figure 7 displays a scatter plot of all the experimental data points of Table 2 from Appendix A fitted with a thin-plate spline curve for data interpolation and smoothing.

**Figure 7**

*Graph 4: Recovered Bioethanol Concentration from Pretreated Corrugated Fibreboard*

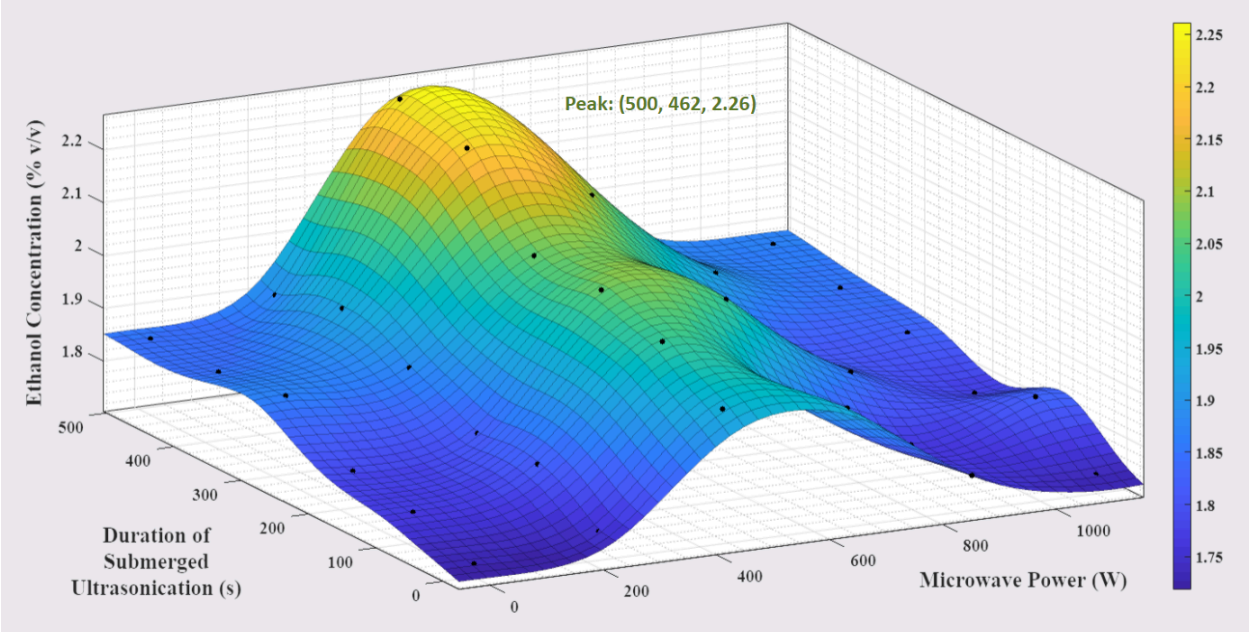


*Note*. The duration and frequency of the MW irradiation was held constant at 8 min and 2,450 MHz, respectively. The frequency and power of the submerged ultrasonication was held constant at 42 kHz and 35.00 W, respectively.

When looking perpendicularly at the xz- and yz-planes of Figure 7, the quadratic and rational equations previously described can be observed, respectively. The peaks of these two-dimensional equations constructively interfere when observed in three dimensions. The point (500, 462, 2.26) is the highest peak of Figure 7, indicating that a power setting of 500 W and a duration of submerged ultrasonication of 462 s theoretically results in the greatest possible bioethanol recovery between these two independent variables. 2.26 ± 0.05% v/v is considerably larger than the peaks of Figures 5 and 6, indicating a synergistic relationship between MW and US irradiation. In addition, this optimal combination recovers an additional 0.53% v/v of bioethanol compared to untreated LCB in this experiment (1.73% v/v). From this peak, Figure 7 reveals a gradual decrease in ethanol concentration along the y-axis and a rapid decrease in both directions along the x-axis. In addition, the data symmetry of the x-axis is much more apparent than that of the y-axis. Further data collection is required to determine whether a greater peak lies further down the y-axis.

For better visualization of the three-dimensional structure of Figure 7, a corresponding contour plot was created. Figure 8 displays the previously-observed plot on a two-dimensional plane using a colour bar to differentiate between the different z-values.

**Figure 8**

*Graph 5: Recovered Bioethanol Concentration from Pretreated Corrugated Fibreboard (Contour Plot)*

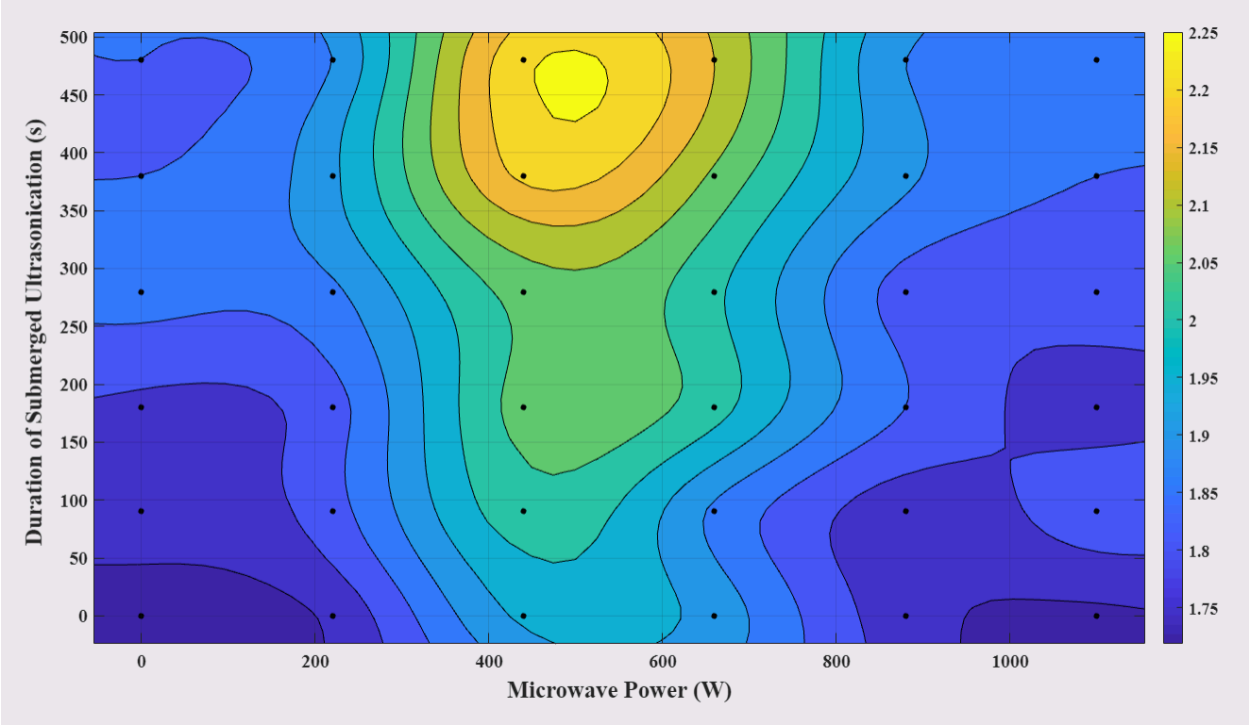


*Note*. The duration and frequency of the MW irradiation was held constant at 8 min and 2,450 MHz, respectively. The frequency and power of the submerged ultrasonication was held constant at 42 kHz and 35.00 W, respectively.

Figure 8 displays an unambiguous peak which likely indicates that a valley exists on all four sides. This contour plot also reveals clear symmetry about a vertical line, likely due to the original quadratic structure of ethanol concentration versus MW power. There are no evident outliers on this plot, indicating the likely absence of data anomalies and/or substantial experimental errors. Overall, this two-dimensional depiction of the independent variables confirms their interdependent effect on ethanol production.

## Discussion

### Conclusions

Due to the crystalline structure of the hemicellulose-lignin matrix of LCB, the pretreatment process is essential to maximizing bioethanol production. An economically- and environmentally-friendly pretreatment method that completely delignifies biomass is yet to be established. This experiment, however, determined a strong, novel correlation between MW and US irradiation as an enhanced method for degrading the recalcitrant

structure of LCB. The digestibility of cellulose following both MW and US irradiation was magnified in comparison to only using one of the independent variables, resulting in improved enzymatic hydrolysis, fermentation, and ultimately, bioethanol recovery.

It was originally hypothesized that the greatest bioethanol recovery of corrugated fibreboard would be achieved at a MW power of 180 W and a duration of submerged ultrasonication of 420 s. Experimentally, however, the greatest bioethanol concentration, 2.24 ± 0.05% v/v, was achieved at a MW power of 440 W and a US duration of 480 s. A thorough analysis of the data collected revealed a theoretical peak of 2.26 ± 0.05% v/v at a MW power of 500 W and a US duration of 462 s.

In retrospect, the predicted duration of submerged ultrasonication that resulted in the greatest bioethanol concentration when combined with MW irradiation was very close to its experimental and theoretical values. The principle of cavitation clearly benefited the pretreatment process, as longer durations of ultrasonication generally resulted in greater yields of bioethanol. It is likely that the submerged medium of the US treatment magnified its positive effects on the delignification of LCB. The threshold at which US-induced protein denaturation occurs, however, remains elusive since no rapid decrease in ethanol concentration along the y-axis of Figure 6 was observed.

The hypothesized MW power, however, was much lower than its experimental and theoretical values. It is likely that the heat produced from the MW irradiation was not enough to break the intermolecular bonds between the glucose subunits in LCB. When increased to a value of 440 W, however, a much greater bioethanol recovery was observed. It was determined that a polynomial equation to the second degree best represents the correlation between MW power and ethanol concentration. The nature of a concave-down parabola further disproves the original hypothesis with respect to the value for MW power. On either side of the vertex, the ethanol concentration decreases toward zero which indicates that too little or too much MW irradiation is damaging to the pretreatment process. The damage caused from too much MW irradiation can likely be attributed to the proportional desiccation of the milled corrugated fibreboard as documented as a qualitative observation in Table 9 of the journal. This heat-induced water evaporation, which was likely caused by the excessive interaction of LCB with an oscillating electromagnetic field, resulted in the amalgamation of the LCB filaments. This reduction in surface area rendered it more difficult for the microwaves to effectively penetrate and fractionate the rigid structure of LCB. Furthermore,

the subsequent process of enzymatic hydrolysis was also adversely affected by the reduced surface area of the agglomerated material. MW power applied in smaller and greater quantities than 500 W has been clearly disproved as an effective lignocellulosic pretreatment method.

**Applications**

Starch-derived biofuels currently yield more ethanol per kilogram of biomass than their lignocellulosic counterparts. The process of refining starch into bioethanol, however, is more costly (Chovau et al., 2013). In fact, the prices of D4 and D6 renewable identification number (RIN) credits—representing biomass-based diesel and corn ethanol, respectively—have been steadily rising over the past few months and are approaching their all-time highest nominal levels (Hill, 2021). As seen on Figure 9, D6 RIN prices, for example, surpassed $1.00 USD per gallon in late January and early February 2021, the highest price since 2013 (Hill, 2021). Low ethanol recovery is the only barrier preventing the widespread adoption of LCB as the new primary source of bioethanol. Overcoming this obstacle would render LCB economically and ecologically superior to starch derivatives.

**Figure 9**

*Graph 6: Daily Spot Prices of D4 and D6 RINs from Jan. 2013–Feb. 2021*


*Note.* Prices are in nominal USD per gallon. Reprinted from *Ethanol and biomass-based diesel RIN prices approaching all-time highs*, by S. Hill, 2021, U.S. Energy Information Administration. Copyright 2021 by U.S. Energy Information Administration.

As previously mentioned, the greatest theoretical bioethanol concentration from milled corrugated fibreboard pretreated with MW and US irradiation was determined to be 2.26 ± 0.05% v/v. Other researchers have

determined the ethanol recovery concentration of untreated starch derivatives to be approximately 2.20% v/v (JoVE, n.d.). This novel lignocellulosic pretreatment method, therefore, results in a bioethanol concentration that is 0.06% v/v greater than untreated starch derivatives. This is a significant discovery since ethanol yields from untreated starch derivatives have historically surpassed those of lignocellulosic sources by about 0.50% v/v (JoVE, n.d.). This increase in bioethanol recovery could render LCB more prosperous than conventional sources of biofuel if adopted on an industrial scale. Further experimentation, as discussed below, is required to identify whether this novel lignocellulosic pretreatment method has the potential to revolutionize the bioethanol production industry.

**Future Research**

Further researching the effects of MW and US irradiation on bioethanol production could confirm and expand upon the current optimal values of these independent variables concluded during this experiment. Additional trials could be conducted at 10 W intervals above and below a MW power setting of 500 W, for example, to further examine the optimal parameters for MW irradiation using this narrowed range. Additional trials could also be conducted to investigate the effects of US duration beyond 480 s on bioethanol production which remains uneasily extrapolatable, largely due to the elusive presence of a threshold at which US-induced protein denaturation occurs. Lastly, this novel pretreatment method could be experimented on other major sources of LCB, like grasses and leaves, to examine its efficacy on a wide-range of materials. Upon further analysis of all these components, this novel lignocellulosic pretreatment method would allow LCB to reach its full potential as a renewable source of bioethanol on an industrial scale.

**Acknowledgements**

We would like to take the opportunity to acknowledge all parties who contributed to the success of our project. Firstly, we would like to offer our utmost gratitude to our teacher supervisor, Mrs. Erin Stewart, for supervising our handling of hazardous chemicals (e.g., 100% v/v ethanol, powdered cellulase, etc.). Furthermore, we would like to express our gratitude to Mr. McCarthy, the head of the Department of Science at St. Ignatius of Loyola Catholic Secondary School, for providing us with the materials required for our experimentation. We would also like to acknowledge Dr. Peter Summers, a professor in the Department of Biology at McMaster University, for recommending ways to refine our final report. Lastly, we would like to acknowledge that the production of our graphs and their corresponding codes is courtesy of the MATLAB software.

**References**

Aftab, M. N., Iqbal, I., Riaz, F., Karadag, A., & Tabatabaei, M. (2019, November 18). *Different Pretreatment Methods of Lignocellulosic Biomass for Use in Biofuel Production*. IntechOpen. https://www.intechopen.com/books/biomass-for-bioenergy-recent-trends-and-future-challenges/different-pretreatment-methods-of-lignocellulosic-biomass-for-use-in-biofuel-production

Agu, O. S., Tabil, L. G., Meda, V., Dumonceaux, T., & Mupondwav, E. (2018, November 5). *Pretreatment of Crop Residues by Application of Microwave Heating and Alkaline Solution for Biofuel Processing: A Review*. IntechOpen. https://www.intechopen.com/books/renewable-resources-and-biorefineries/pretreatment-of-crop-residues-by-application-of-microwave-heating-and-alkaline-solution-for-biofuel-

Akhtar, N., Gupta, K., Goyal, D., & Goyal, A. (2016). Recent advances in pretreatment technologies for efficient hydrolysis of lignocellulosic biomass. *Environmental Progress & Sustainable Energy, 35*, 489–511. https://doi.org/10.1002/ep.12257

Arora, A., Nandal, P., Singh, J., & Verma, M. L. (2020, January 8). *Nanobiotechnological advancements in lignocellulosic biomass pretreatment*. ScienceDirect. https://www.sciencedirect.com/science/article/pii/S2589299120300021#b0100

AVCalc LLC. (n.d.). *Density of Leavening agents, yeast, baker's, active dry (food)*. https://www.aqua-calc.com/page/density-table/substance/leavening-blank-agents-coma-and-blank-yeast-coma-and-blank-baker-quote-s-coma-and-blank-active-blank-dry

Azhar, S., Rahmath, A., Jambo, S., Marbawi, H., Gansau, J., Faik, A., & Rodrigues, K. (2017, July). *Yeasts in sustainable bioethanol production: A review*. ScienceDirect. https://www.sciencedirect.com/science/article/pii/S2405580816302424

Baruah, J., Nath, B. K., Sharma, R., Kumar, S., Chandra, R., Baruah, D. C., & Kalita, E. (2018, December 18). Recent Trends in the Pretreatment of Lignocellulosic Biomass for Value-Added Products. *Frontiers in Energy Resea*rch. https://doi.org/10.3389/fenrg.2018.00141

Boshoff, S., Gottumukkala, L., van Rensburg, E., & Görgens, J. (2015). Paper sludge (PS) to bioethanol: Evaluation of virgin and recycle mill sludge for low enzyme, high-solids fermentation. *National Center for Biotechnology Information, 203,* 103–111. https://doi.org/10.1016/j.biortech.2015.12.028

Cardboard Balers. (2017, December 19). *Amazing Facts About Cardboard Waste and Recycling*. https://www.cardboardbalers.org/cost-agricultural-solar-panels/#:~:text=In%20the%20United%20States%2C%20850,year%20in%20paper%20and%20cardboard

Celignis Biomass Analysis Laboratory. (n.d.-a). *Bioethanol From the Fermentation Of Biomass-Derived Sugars*. https://www.celignis.com/fermentation-to-bioethanol.php

Celignis Biomass Analysis Laboratory. (n.d.-b). *Biomass Chemistry*. https://www.celignis.com/chemistry.php

Chen, H., Liu, J., Chang, X., Chen, D., Xue, Y., Liu, P., Lin, H., & Han, S. (2017). A review on the pretreatment of lignocellulose for high-value chemicals. *Fuel Processing Technology, 160*, 196–206. https://doi.org/10.1016/j.fuproc.2016.12.007

Cherpozat, L., Loranger, E., & Daneault, C. (2017). Ultrasonic pretreatment effects on the bio-oil yield of a laboratory-scale slow wood pyrolysis. *Journal of Analytical and Applied Pyrolysis, 126*, 31–38. https://doi.org/10.1016/j.jaap.2017.06.027

Chovau, S., Degrauwe, D., & Van der Bruggen, B. (2013). Critical analysis of techno-economic estimates for the production cost of lignocellulosic bio-ethanol. *Renewable and Sustainable Energy Reviews, 26*, 307–321. https://doi.org/10.1016/j.rser.2013.05.064

Dashko, S., Zhou, N., Compagno, C., & Piškur, J. (2014). Why, when, and how did yeast evolve alcoholic fermentation? *FEMS Yeast Research, 14*(6), 826–832. https://doi.org/10.1111/1567-1364.12161

del Río, J. C., Rencoret, J., Prinsen, P., Martínez, Á. T., Ralph, J., & Gutiérrez, A. (2012). Structural Characterization of Wheat Straw Lignin as Revealed by Analytical Pyrolysis, 2D-NMR, and Reductive Cleavage Methods. *Journal of Agricultural and Food Chemistry, 60*(23), 5922–5935. https://doi.org/10.1021/jf301002n

Den, W., Sharma, V. K., Lee, M., Nadadur, G., & Rajender, V. S. (2018, April 27). Lignocellulosic Biomass Transformations via Greener Oxidative Pretreatment Processes: Access to Energy and Value-Added Chemicals. *Frontiers in Chemistry*. https://www.frontiersin.org/articles/10.3389/fchem.2018.00141/full

Gupta, R., Mehta, G., Deswal, D., Sharma, S., Jain, K. K., Kuhad, R. C., & Singh, A. (2013). *Biotechnology for Environmental Management and Resource Recovery.* Springer. https://doi.org/10.1007/978-81-322-0876-1

Gurgel, L. V., Junior, O. K., Gil, R. P., & Gil, L. F. (2008). Adsorption of Cu(II), Cd(II), and Pb(II) from aqueous single metal solutions by cellulose and mercerized cellulose chemically modified with succinic anhydride. *Bioresource Technology, 99*(8), 3077–3083. https://doi.org/10.1016/j.biortech.2007.05.072

Hill, S. (2021, February 24). *Ethanol and biomass-based diesel RIN prices approaching all-time highs*. U.S. Energy Information Administration. https://www.eia.gov/todayinenergy/detail.php?id=46876

Hokkanen, S., Repo, E., & Sillanpää, M. (2013). Removal of heavy metals from aqueous solutions by succinic anhydride modified mercerized nanocellulose. *Chemical Engineering Journal, 223*, 40–47. https://doi.org/10.1016/j.cej.2013.02.054

Hussain, A., Arif, S. M., & Aslam, M. (2017). Emerging renewable and sustainable energy technologies: State of the art. *Renewable and Sustainable Energy Reviews, 71*, 12–28. https://doi.org/10.1016/j.rser.2016.12.033

Ivetic, D., Omorjan, R., Djordjevic, T., & Antov, M. (2017). The impact of ultrasound pretreatment on the enzymatic hydrolysis of cellulose from sugar beet shreds: Modeling of the experimental results. *Environmental Progress & Sustainable Energy, 36*(4). https://doi.org/10.1002/ep.12544

Journal of Visualized Experiments. (n.d.). *Biofuels: Producing Ethanol from Cellulosic Material*. https://www.jove.com/v/10014/biofuels-producing-ethanol-from-cellulosic-material

Kerns, M. (n.d.). *What Is Nutritional Yeast at the Grocery Store?* SFGATE. https://healthyeating.sfgate.com/nutritional-yeast-grocery-store-1287.html

Khajavi, R., Atlasi, A., & Yazdanshenas, M. E. (2013). Alkali treatment of cotton yarns with ultrasonic bath. *Textile Research Journal, 83*(8), 827–835. https://doi.org/10.1177/0040517512467077

Kumar, A. K., & Sharma, S. (2017). Recent updates on different methods of pretreatment of lignocellulosic feedstocks: a review. *Bioresources and Bioprocessing, 4*(7). https://doi.org/10.1186/s40643-017-0137-9

Kuna, E., Behling, R., Valange, S., Chatel, G., & Colmenares, J. C. (2017, March 23). *Sonocatalysis: A Potential Sustainable Pathway for the Valorization of Lignocellulosic Biomass and Derivatives*. Springer Nature. https://link.springer.com/article/10.1007/s41061-017-0122-y

Liu, Y., Sun, B., Zheng X., Yu, L., & Li, J. (2018). Integrated microwave and alkaline treatment for the separation between hemicelluloses and cellulose from cellulosic fibers. *Bioresource Technology, 247*, 859–863. https://doi.org/10.1016/j.biortech.2017.08.059

Loow, Y. L., Wu, T. Y., Tan, K. A., Lim, Y. S., Siow, L. F., Jahim, J., Mohammad, A. W., & Teoh, W. H. (2015). Recent Advances in the Application of Inorganic Salt Pretreatment for Transforming Lignocellulosic Biomass into Reducing Sugars. *Agricultural and Food Chemistry, 63*, 8349–8363. https://doi.org/10.1021/acs.jafc.5b01813

Luzzi, S. C., Artifon, W., Piovesan, B., Tozetto, E., Mulinari, J., Kuhn, G. O., Mazutti, M. A., Priamo, W. L., Mossi, A. J., Silva, M. F., Golunski, S. M., Treichel, H., & Bender, J. P. (2017). Pretreatment of lignocellulosic biomass using ultrasound aiming at obtaining fermentable sugar. *Biocatalysis and Biotransformation, 35*(3), 166–167. https://doi.org/10.1080/10242422.2017.1310206

Ma, Y., Hummel, M., Määttänen, M., Särkilahti, A., Harlin, A., & Sixta, H. (2015). Upcycling of waste paper and cardboard to textiles. *Green Chemistry, 18*, 856–866. https://doi/org/10.1039/C5GC01679G

McParland, J. J., Grethlein, H. E., & Converse, A. O. (2003). Kinetics of acid hydrolysis of corn stover. *Solar Energy, 28*(1), 55–63. https://doi.org/10.1016/0038-092X(82)90224-9

Mussatto, S. I., & Dragone, G. M. (2016). *Biomass Fractionation Technologies for a Lignocellulosic Feedstock Based Refinery*. Elsevier Inc. https://doi.org/10.1016/B978-0-12-802323-5.00001-3

Ni, J., Na, H., She, Z., Wang, J., Xue, W., & Zhu, J. (2014). Responsive behavior of regenerated cellulose in hydrolysis under microwave radiation. *Bioresource Technology, 167*, 69–73. https://doi.org/10.1016/j.biortech.2014.05.066

Oliva, J. M., Negro, M. J., Manzanares, P., Ballesteros, I., Chamorro, M. Á., Sáez, F., Ballesteros, M., & Moreno, A. D. (2017). A Sequential Steam Explosion and Reactive Extrusion Pretreatment for Lignocellulosic Biomass Conversion Within a Fermentation-Based Biorefinery Perspective. *Fermentation, 3*(2), 15. https://doi.org/10.3390/fermentation3020015

Peng, H., Li, H., Luo, H., & Xu, J. (2013). A novel combined pretreatment of ball milling and microwave irradiation for enhancing enzymatic hydrolysis of microcrystalline cellulose. *Bioresource Technology, 130*, 81–87. https://doi.org/10.1016/j.biortech.2012.10.167

Ravichandran, A., & Sridhar, M. (2016). Versatile peroxidases: super peroxidases with potential biotechnological applications—a mini review. *Journal of Dairy, Veterinary & Animal Research, 4*(2), 277–280. https://doi.org/10.15406/jdvar.2016.04.00116

Ritter, S. K. (2014). Microwave Chemistry Remains Hot, Fast, And A Tad Mystical. *Chemical & Engineering News, 92*(4). https://cen.acs.org/articles/92/i4/Microwave-Chemistry-Remains-Hot-Fast.html

Saifuddin, N. M., Hussain, R., & Palanisamy, K. (2013). Microwave-Assisted Alkaline Pretreatment and Microwave Assisted Enzymatic Saccharification of Oil Palm Empty Fruit Bunch Fiber for Enhanced Fermentable Sugar Yield. *Journal of Sustainable Bioenergy Systems, 3*(1), 7–17. https://doi.org/10.4236/jsbs.2013.31002

Su, J., Zhu, H., Wang, L., Liu, X., Nie, S., & Xiong, J. (2016). Optimization of Microwave-Hydrogen Peroxide Pretreatment of Cellulose. *BioResources, 11*(3). https://doi.org/10.15376/biores.11.3.7416-7430

Sun, R., & Tomkinson, J. (2002). Comparative study of lignins isolated by alkali and ultrasound-assisted alkali extractions from wheat straw. *Ultrasonics Sonochemistry, 9*(2), 85–93. https://doi.org/10.1016/S1350-4177(01)00106-7

Sun, S., Sun, S., Cao, X., & Sun, R. (2016). The Role of Pretreatment in Improving the Enzymatic Hydrolysis of Lignocellulosic Materials. *Bioresource Technology, 199*, 49–58. https://doi.org/10.1016/j.biortech.2015.08.061

Ulin, D. (2011, October 27). *How Sound Waves Work Underwater*. Indiana Public Media. https://indianapublicmedia.org/amomentofscience/sound-waves-work-underwater.php

Wang, L., Sharifzadeh, M., Templer, R., & Murphy, R. J. (2012). Technology performance and economic feasibility of bioethanol production from various waste papers. *Energy Environ. Sci., 5*, 5717–5730. https://doi.org/10.1039/c2ee02935a

Wang, X., Cheng, S., Li, Z., Men, Y., & Wu, J. (2020). Impacts of Cellulase and Amylase on Enzymatic Hydrolysis and Methane Production in the Anaerobic Digestion of Corn Straw. *Sustainability, 12*(13), 5453. https://doi.org/10.3390/su12135453

Wi, S. G., Cho, E. J., Lee, D.-S., Lee, S. J., Lee, Y. J., & Bae, H.-J. (2015). Lignocellulose conversion for biofuel: a new pretreatment greatly improves downstream biocatalytic hydrolysis of various lignocellulosic materials. *Biotechnology for Biofuels, 8*(228). http://dx.doi.org/10.1186/s13068-015-0419-4

Xu, C., & Ferdosian, F. (2017). *Conversion of Lignin into Bio-Based Chemicals and Materials*. Springer Nature. https://doi.org/10.1007/978-3-662-54959-9

Yue, F., Lan, W., Zhang, A., Liu, C., Sun, R., & Ye, J. (2012). Dissolution of Holocellulose in Ionic Liquid Assisted with Ball-Milling Pretreatment and Ultrasound Irradiation. *BioResources, 7*(2). https://ojs.cnr.ncsu.edu/index.php/BioRes/article/view/BioRes_07_2_2199_Dissolution_Holocellulose_Ionic_Liquid_Ball_Mill_Ultrasound

Zhou, S., Raouche, S., Grisel, S., Sigoillot, J., and Herpoël-Gimbert, I. (2017). Efficient biomass Pretreatment using the White-rot fungus *Polyporus brumalis*. *Fungal Genomics and Biology, 7*(1). https://doi.org/10.4172/2165-8056.1000150

## Appendix A: Raw Data Collection

Table 1 contains the data collected while completing an error analysis of ethanol concentration in solution. The mean percent deviation of the theoretical and experimental values was calculated to be 2.1%.

**Table 1**

*Percent Deviation of Ethanol Concentration in Solution*

| Theoretical Ethanol Concentration (% v/v) | Experimental Ethanol Concentration (% v/v) | Percent Deviation (%) |
|---|---|---|
| 0.25 | 0.26 | 4.0 |
| 0.50 | 0.50 | 0.0 |
| 0.75 | 0.72 | 4.0 |
| 1.00 | 0.99 | 1.0 |
| 1.25 | 1.28 | 2.40 |
| 1.50 | 1.47 | 2.00 |
| 1.75 | 1.71 | 2.29 |
| 2.00 | 2.03 | 1.50 |

*Note*. The mean percent deviation is 2.1%.

Table 2 contains the resulting ethanol concentrations of the samples collected during the third day of the experimental procedure. Note that the values for ethanol concentration were collected during formal experimentation of the independent variables and, therefore, do not represent mean averages but rather highly-accurate single readings. Further details about this subject can be found in the journal.

**Table 2**

*Recovered Bioethanol Concentration from Pretreated Corrugated Fibreboard*

| Microwave Power (W) | Duration of Submerged Ultrasonication (s) | Ethanol Concentration (% v/v) |
|---|---|---|
| 0 | 0 | 1.73 |
| | 90 | 1.77 |
| | 180 | 1.79 |

| Microwave Power (W) | Duration of Submerged Ultrasonication (s) | Ethanol Concentration (% v/v) |
|---|---|---|
| 0 | 280 | 1.87 |
| | 380 | 1.85 |
| | 480 | 1.85 |
| 220 | 0 | 1.76 |
| | 90 | 1.83 |
| | 180 | 1.83 |
| | 280 | 1.89 |
| | 380 | 1.94 |
| | 480 | 1.90 |
| 440 | 0 | 1.96 |
| | 90 | 2.03 |
| | 180 | 2.07 |
| | 280 | 2.07 |
| | 380 | 2.21 |
| | 480 | 2.24 |
| 660 | 0 | 1.93 |
| | 90 | 1.89 |
| | 180 | 2.02 |
| | 280 | 2.01 |
| | 380 | 2.09 |
| | 480 | 2.15 |
| 880 | 0 | 1.77 |
| | 90 | 1.77 |
| | 180 | 1.85 |
| | 280 | 1.83 |
| | 380 | 1.91 |

| Microwave Power (W) | Duration of Submerged Ultrasonication (s) | Ethanol Concentration (% v/v) |
|---|---|---|
| 880 | 480 | 1.90 |
| 1,100 | 0 | 1.74 |
| | 90 | 1.83 |
| | 180 | 1.78 |
| | 280 | 1.83 |
| | 380 | 1.85 |
| | 480 | 1.87 |

## Appendix B: Photographs

**Figure 10**

*Day 1, Steps 1–3: Personal Protective Equipment (PPE)*


*Note.* The PPE used for this experiment includes a dry-chemical fire extinguisher, two pairs of eye goggles, and eighteen pairs of nitrile powder free gloves.

**Figure 11**

*Day 1, Step 7: Square Prisms of Corrugated Fibreboard*

*Note.* The primary source of lignocellulosic biomass for this experiment is corrugated fibreboard. Seventy-five 2 cm x 2 cm x 0.4 cm square prisms of corrugated fibreboard are cut out from the initial sheet measuring 15 cm x 20 cm x 0.4 cm.

**Figure 12**

*Day 1, Step 9: Submerged Square Prisms of Corrugated Fibreboard*

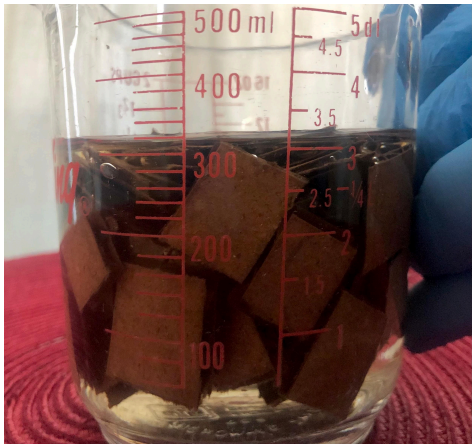


*Note.* The square prisms of corrugated fibreboard are submerged in 300. mL of water for approximately thirty seconds.

**Figure 13**

*Day 1, Step 11: Pre-Processed Corrugated Fibreboard*


*Note.* The square prisms of corrugated fibreboard are placed in the base of the Braun Multimix Food Processor prior to being processed for ten minutes.

**Figure 14**

*Day 1, Step 12: Post-Processed Corrugated Fibreboard*

*Note.* The corrugated fibreboard in the base of the food processor has been processed for ten minutes.

**Figure 15**

*Day 1, Steps 13–14: Post-Processed Corrugated Fibreboard with Added Water*


*Note.* 250. mL of steam-distilled, ozonated water is poured into the base of the food processor with the processed corrugated fibreboard.

**Figure 16**

*Day 1, Step 14: Post-Processed Corrugated Fibreboard Following Reprocessing*

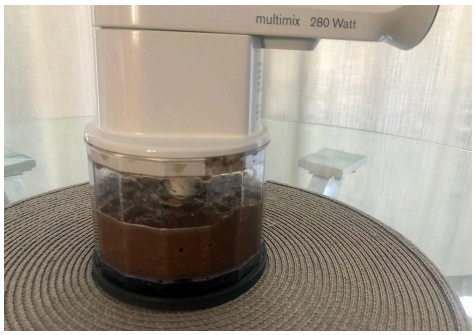


*Note.* The processed corrugated fibreboard with added water is processed on the highest power setting for an additional five minutes.

**Figure 17**

*Day 1, Step 19: Weighing of Milled Corrugated Fibreboard*


*Note.* 17.00 g of milled corrugated fibreboard is placed into each 30-mL glass vial.

**Figure 18**

*Day 1, Steps 21, 39: Milled Corrugated Fibreboard In Glass Vials (Group A Samples)*

*Note.* The milled corrugated fibreboard is placed into twelve glass vials, all of which belong to the samples of Group A (MW: 100%, 80%; US: 480. s, 380. s, 280. s, 180. s, 90. s, 0 s).

**Figure 19**

*Day 1, Steps 22, 39: Microwave Irradiation*

*Note.* Selected samples of Group A are microwaved at 100% or 80% power for a duration of eight minutes.

**Figure 20**

*Day 1, Steps 28, 38: Submerged Ultrasonication*


*Note.* Selected samples of Group A undergo submerged ultrasonication at 42 kHz for a duration of 480. s, 380. s, 280. s, 180. s, or 90. s.

**Figure 21**

*Day 1, Steps 37, 39: Labelled Erlenmeyer Flasks with Pretreated Corrugated Fibreboard*

*Note.* The corrugated fibreboard transferred into the twelve Erlenmeyer flasks of Group A underwent different pretreatment parameters.

**Figure 22**

*Day 1, Step 45: Weighing of Powdered Cellulase*


*Note.* Powdered cellulase is transferred onto the electronic balance using a scoopula until it reads 0.35 g.

**Figure 23**

*Day 1, Step 49: Stirring of Powdered Cellulase in Erlenmeyer Flask*

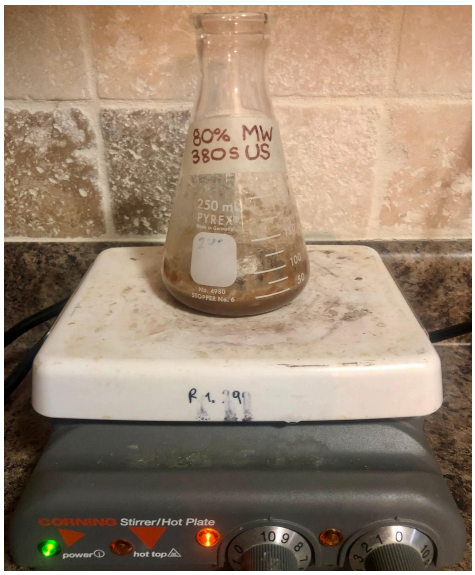

*Note.* 0.35 g of powdered cellulase is transferred to each of the Erlenmeyer flasks and mixed thoroughly for five minutes by way of the Corning PC–420 Laboratory Stirrer on the highest setting.

**Figure 24**

*Day 1, Step 54: Pre-Incubation of (Night 1)*


*Note.* Once the incubator reaches a temperature of 40. ℃, the twelve Erlenmeyer flasks from Group A are placed inside for a period of twenty-four hours.

**Figure 25**

*Day 2, Step 4: Post-Incubation (Night 1)*

*Note.* The twelve Erlenmeyer flasks are ready to be removed from the incubator after being heated for a period of twenty-four hours during the first night.

**Figure 26**

*Day 2, Step 7: Weighing of Saccharomyces cerevisiae*


*Note. Saccharomyces cerevisiae* is transferred onto the electronic balance using a scoopula until it reads 5.30 g.

**Figure 27**

*Day 2, Step 12: Stirring of Saccharomyces cerevisiae in Erlenmeyer Flask*

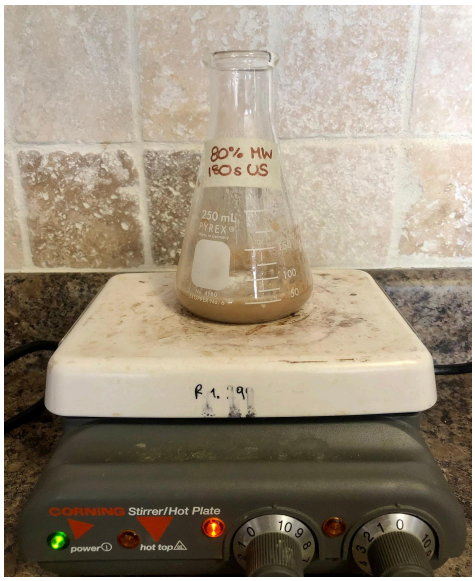

*Note.* 5.3 g of *Saccharomyces cerevisiae* is transferred to each of the Erlenmeyer flasks and mixed thoroughly for five minutes by way of the Corning PC–420 Laboratory Stirrer on the highest setting.

**Figure 28**

*Day 2, Step 15: Erlenmeyer Flask with Attached Airlock*

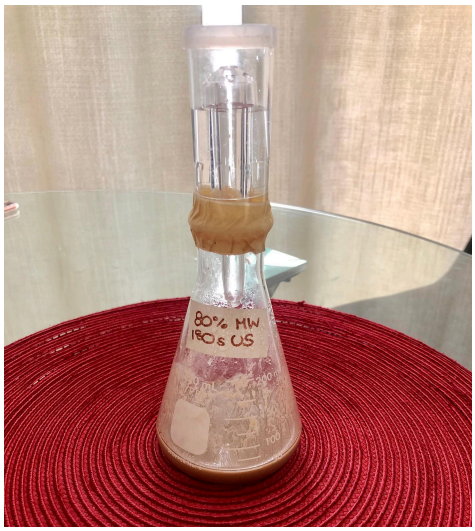


*Note.* To allow for the accumulation of ethanol gas, an airlock is secured on each of the twelve Erlenmeyer flasks with masking tape.

**Figure 29**

*Day 2, Step 19: Pre-Incubation (Night 2)*


*Note.* Once the incubator is adjusted to a temperature of 40. ℃ if necessary, the twelve Erlenmeyer flasks from Group A are placed inside a second time for a period of twenty-four hours.

**Figure 30**

*Day 3, Step 5: Post-Incubation (Night 2)*


*Note.* The twelve Erlenmeyer flasks are ready to be removed from the incubator after being heated for a period of twenty-four hours during the second night.

**Figure 31**

*Day 3, Step 5: Cool-Down Period of Erlenmeyer Flask*


*Note.* The twelve Erlenmeyer flasks are cooled for a period of approximately one hour after being removed from the incubator for the second time.

**Figure 32**

*Day 3, Step 12: 35 mL of 1% v/v Ethanol Solution*


*Note.* 34.65 mL of steam-distilled, ozonated water is added to 0.35 mL of a 100% v/v solution of ethanol to form 35 mL of a 1% v/v solution of ethanol.

**Figure 33**

*Day 3, Step 19: Calibration of the PASPORT Ethanol Sensor*

*Note.* With the probe of the PASPORT Ethanol Sensor placed 1 cm above the solution, the 1% CAL button is pressed for four seconds to calibrate the sensor.

**Figure 34**

*Day 3, Step 23: Detection of Ethanol in Erlenmeyer Flask*

*Note.* The ethanol concentration of the Erlenmeyer flask is measured by the PASPORT Ethanol Sensor and displayed on the SPARK Science Learning System.

**Figure 35**

*Days 1–3: Display of All Materials*


*Note.* All materials used in the method, with the exception of large appliances, are displayed above. Please refer to the *Materials* section of the report for a complete list.